Investigating Material Approximations in Spacecraft Radiation Analysis

Steven A. Walker[1], Tony C. Slaba[2], Martha S. Clowdsley[2], Steve R. Blattnig[2]

[1] *Old Dominion University, Norfolk, VA*
[2] *NASA Langley Research Center, Hampton, VA*

Abstract

During the design process, the configuration of space vehicles and habitats changes frequently and the merits of design changes must be evaluated. Methods for rapidly assessing astronaut exposure are therefore required. Typically, approximations are made to simplify the geometry and speed up the evaluation of each design. In this work, the error associated with two common approximations used to simplify space radiation vehicle analyses, scaling into equivalent materials and material reordering, are investigated. Over thirty materials commonly found in spacesuits, vehicles, and human bodies are considered. Each material is placed in a material group (aluminum, polyethylene, or tissue), and the error associated with scaling and reordering was quantified for each material. Of the scaling methods investigated, range scaling is shown to be the superior method, especially for shields less than 30 g/cm^2 exposed to a solar particle event. More complicated, realistic slabs are examined to quantify the separate and combined effects of using equivalent materials and reordering. The error associated with material reordering is shown to be at least comparable to, if not greater than, the error associated with range scaling. In general, scaling and reordering errors were found to grow with the difference between the average nuclear charge of the actual material and average nuclear charge of the equivalent material. Based on this result, a different set of equivalent materials (titanium, aluminum, and tissue) are substituted for the commonly used aluminum, polyethylene, and tissue. The realistic cases are scaled and reordered using the new equivalent materials, and the reduced error is shown.

1. Introduction

Space radiation analyses of complex vehicle or habitat geometries are often performed by interpolating over a database of dose or dose equivalent values in order to integrate over the shielding distribution representing the vehicle or habitat. The first step in this process is to choose a set of materials and specify their order. A commonly used choice is an aluminum structure followed by a polyethylene shield and tissue. Ray tracing techniques are then used to determine the amount of tissue and shielding material along each of a large number of rays covering the full 4π steradians emanating from the specified target point and terminating at the exterior surface of the vehicle. Figure 1 is an example of this ray tracing process. The grey lines are part of a model of the International Space Station (ISS). From a central point left of the center of Figure 1, the rays emanate outward to cover the full sphere. The red lines are the intersection of each ray with a solid vehicle element. For each material traversed that does not match the predefined list of materials, scaling methods are used to convert the given material thickness to a thickness of the appropriate material. These scaling methods, which are often referred to as using equivalent materials (e.g. equivalent aluminum scaling or equivalent aluminum approximation), are used to keep the dimensions of the interpolation database to a manageable number.

The next step in this process is to analyze the distribution of thicknesses generated by the ray tracing procedure and use a transport code such as HZETRN (High charge (Z) and Energy TRaNsport) [Wilson et al. 1991; Wilson et al. 2005; Slaba et al. 2010] to generate a dose versus depth database encompassing the chosen materials and depths. The dose values for each of the ray traced shield and target thicknesses are computed by interpolating over the dose versus depth database. Dose at a point is calculated by integrating over all the rays emanating from that point. This procedure is the same for any other response, be it dose equivalent, flux, or Linear Energy Transfer (LET), etc. This procedure enables rapid assessment of astronaut exposure and has been used to analyze the ISS, the Orion module of the Crew Exploration Vehicles (CEV), and a variety of other space vehicles and habitats.

Badavi et al. [2010] have already studied some of the errors associated with materials scaling. In that work, it was concluded that converting hydrogen rich polymers into equivalent aluminum was not appropriate for highly energetic solar particle events (SPE) or galactic cosmic ray (GCR) spectra based on flux and dose comparisons for a limited number of materials. In this work, a more comprehensive set of materials are studied (high Z metals, polymers, body tissues, etc.) with multiple equivalent materials. The effect of material reordering is also investigated. Dose equivalent is examined due to its importance in assessing biological risks, and realistic slabs that may be found in spacecraft geometries with anywhere from 3-40 layers are studied.

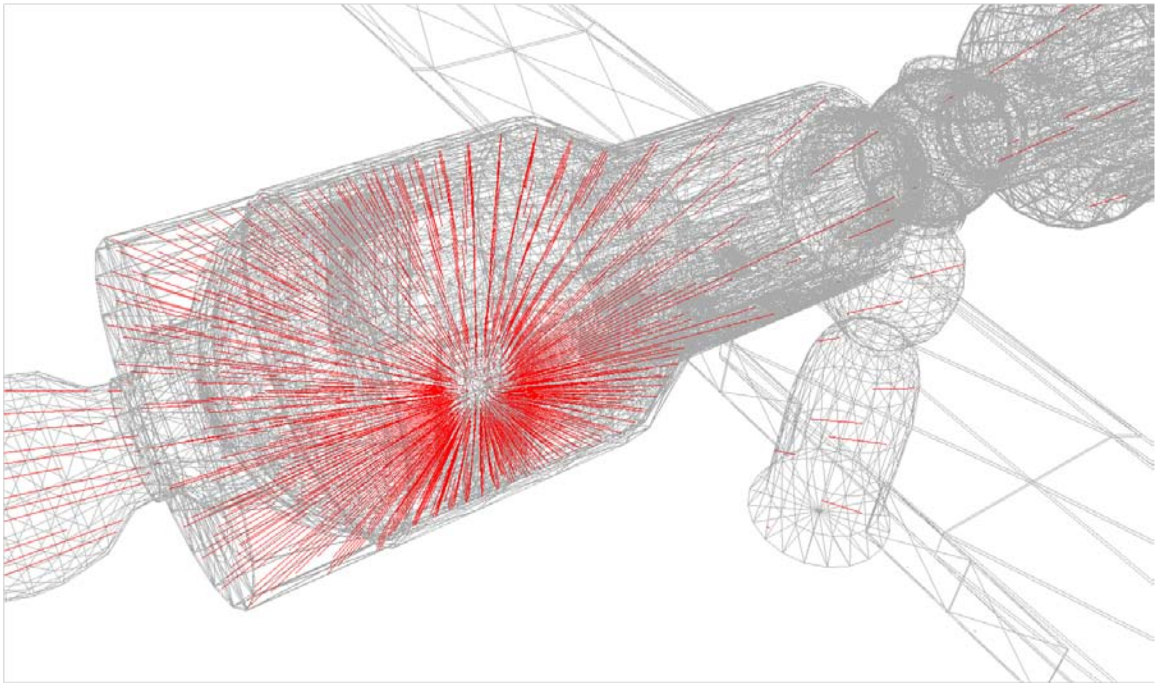

Figure 1. Example ray trace using a model of the ISS (grey lines). The red lines are the intersections of each ray with solid model elements. Figure courtesy of Garry Qualls, NASA Langley Research Center.

The first objective of this work is to investigate the error associated with converting materials into equivalent aluminum, polyethylene, and tissue. These equivalent materials are being examined because they have been used extensively in the past. The second objective is to examine the errors caused by reordering materials. Reordering refers to the process where all materials converted to equivalent aluminum are summed and transported through first, all materials converted to equivalent polyethylene are summed and transported through second, and materials converted to equivalent tissue are transported through last. This process occurs frequently in vehicles and human body models where a ray may traverse many materials in the geometry. The third objective is to examine the combined effects of scaling and material reordering. Finally, based on these results, new equivalent materials are suggested and the reduced errors associated with the new materials are shown. In this paper, the space radiation environments used were the King parameterization of the August 1972 SPE [King 1974] and the 1977 GCR solar minimum environment, based on the 2006 Badhwar-O'Neill model [O'Neill et al. 2006].

2. Analysis Description

2.1 Effects of Converting to Equivalent Aluminum, Polyethylene, and Tissue

This section addresses the effects of mapping materials into equivalent thicknesses of aluminum, polyethylene, and tissue. The term "equivalent material" is used frequently throughout the rest of the text. An amount of equivalent material is the amount of that material that is assumed to have approximately the same shielding properties as a given amount of another material. For example, thickness X of stainless steel would be converted into thickness Y of equivalent aluminum. In this paper, thickness is expressed in terms of areal density units of g/cm^2. This is the length (cm) multiplied by the density (g/cm^3) of the material. Two methods of scaling are investigated: equal thickness scaling and range scaling.

Three material groups are chosen: an aluminum group (A), a polyethylene group (P), and a tissue group (T). Each group represents an equivalent material that is often used in the interpolation procedure described in the introduction. Several materials commonly used to represent the human body, spacesuits, vehicles, and habitats are then systematically placed into one or more of these groups. A material is defined to be in the equivalent aluminum group if the range of a 50 MeV proton (R_{50}) in that material was greater than 2.8 g/cm^2. A material is defined to be in the equivalent polyethylene group if the R_{50} value in that material was less than 2.8 g/cm^2. See Badavi et al. [2010] for a discussion of the R_{50} values in material scaling. Carbon, fiberglass, and Teflon, with ranges between 2.5 g/cm^2 and 2.8 g/cm^2 are placed in both the aluminum and polyethylene groups due to the proximity of their R_{50} values to the delimiting value of 2.8 g/cm^2. The R_{50} value for neoprene is also close to 2.5 g/cm^2, but unlike carbon, fiberglass, and Teflon, neoprene contains hydrogen. Based on Badavi et al. [2010], this hydrogen containing polymer is not included in the aluminum group. The tissue group contains various bone and generic tissue compositions found in the human body, irrespective of their R_{50} value. The R_{50} value is used to define groups for various materials because this value has been historically used in what is called "range scaling." More will be said about this scaling method later in this section. The use of 2.8 g/cm^2 as a delimiting value was motivated by simultaneously comparing the dose and dose equivalent versus depth curves with the R_{50} values for the various materials. The dose and dose equivalent curves will be discussed in Section 3.1. A complete list of the materials examined in this paper along with their R_{50} values and range scaling ratios, ρ, can be found in Table 1. The range scaling ratio for a material is the ratio of the R_{50} value for the equivalent material to the R_{50} value for the actual material. More will be said about this ratio below and in Section 3.1.

Table 1. Materials in the aluminum (A), polyethylene (P), and tissue (T) groups with their R_{50} and range scaling values. Carbon, fiberglass, and Teflon are in the aluminum and polyethylene groups.

Group	Material Name	R_{50} (g/cm^2)	ρ
A	Aluminum	2.920	1.000
A	Al-Li 2090	2.927	0.997
A	Aluminum 7075	2.953	0.989
A/P	Carbon	2.485	1.175/0.830
A	Copper	3.557	0.821
A/P	Fiberglass	2.687	1.087/0.768
A	Stainless Steel	3.353	0.871
A/P	Teflon	2.726	1.071/0.757
A	Titanium	3.284	0.889
A	Tufi	2.800	1.043
P	Polyethylene	2.063	1.000
P	IM7/977-3 Graphite Epoxy	2.267	0.910
P	Kevlar	2.360	0.874
P	Mylar	2.372	0.870
P	Neoprene	2.444	0.844
P	Neoprene Ripstop	2.239	0.922
P	Nylon	2.193	0.941
P	Nylon/Spandex	2.268	0.910
P	Orthofabric	2.609	0.791
P	Polycarbonate	2.319	0.890
P	Polysulfone	2.351	0.877
P	Spandex	2.288	0.902
P	Urethane Ripstop	2.210	0.933
T	Tissue	2.220	1.000
T	Adipose	2.153	1.031
T	Average Bone	2.369	0.937
T	Cartilage	2.247	0.988
T	Cortical Bone	2.524	0.879
T	Lung	2.220	1.000
T	Muscle	2.221	0.999
T	Skin	2.221	1.000
T	Soft Tissue	2.208	1.005

There are two scaling methods considered in this section. Equal thickness scaling is an approximation where an equivalent material is substituted for a specific material of equal thickness. For example, 5 g/cm^2 of stainless steel is directly approximated with 5 g/cm^2 of equivalent aluminum. In order to quantify the error introduced by the equal thickness approximation for these materials, dose and dose equivalent values are computed at various depths in each of the materials within each group, and the difference between the results for the actual material and the results for the corresponding equivalent material is calculated. Dose equivalent is computed based on the ICRP (International Commission on Radiological Protection) 60 quality factor [ICRP 1990].

In range scaling, the thickness of a given material is multiplied by a scaling factor to obtain the appropriate thickness of the equivalent material. This scale factor, ρ, is the ratio of the R_{50} value in the equivalent material to the R_{50} value in the specific material [Badavi et al. 2010]. The range scaling values for each material in each group are given in Table 1. The error introduced by range scaling is determined by comparing dose values at given depths in the actual material to the dose value at corresponding range scaled depths in the equivalent material.

2.2 Effects of Reordering Materials

In this section, the error associated with reordering materials in the interpolation procedure described in the introduction is examined. In a full vehicle geometry, materials mapped into equivalent aluminum (A), polyethylene (P), or tissue (T) are frequently reordered so that the final slab thicknesses for each ray appear in the same order as the dose or dose equivalent interpolation database, for example: APT. Due to the broad distribution of materials, number of layers, and thicknesses that are generated from complex geometries, it is difficult to precisely determine the error associated with reordering equivalent materials. However, some useful statements can be made for specific materials by considering a distribution of thicknesses and number of layers. In order to quantify the error associated with reordering aluminum (A), polyethylene (P), and tissue (T), slabs of thickness 1 g/cm^2, 10 g/cm^2, 50 g/cm^2, and 100 g/cm^2 were considered. The slabs were split into 2, 4, 8, 16, 32, and 64 layers of alternating A and P, A and T, or P and T. Dose and dose equivalent values at the end of each slab are calculated. In each case, the results behind the multi-layer arrangements are compared to the 2-layer results. This convention was chosen because in the interpolation and ray-tracing procedure described in the introduction, multi-layer slabs of AP, AT, or PT are collapsed and reordered to 2-layer slabs. This analysis is used to determine how reordering error depends on slab thickness and number of layers being reordered.

2.3 Combined Effects of Scaling and Reordering in Realistic Slabs

The previous two sections discussed separately the effects of scaling materials and reordering materials in simplified slabs. In this section, the combined effects of material scaling and reordering will be examined in complex multi-layer slabs made up of historically used space materials. Due to the number of approximations being made to reduce the complex multi-layer slabs to equivalent materials, several comparisons are made so that the effect of each approximation can be quantified separately. First, the results (dose and dose equivalent) behind the original multi-layer slab are compared with the scaled slab (scaling error). Next, the scaled slab results are compared with the scaled, reordered slab results (reordering error). Last, the original slab results are compared with the scaled, reordered slab results (combined effects of scaling and reordering). Based on the results in the previous sections, alternative equivalent materials are substituted for the commonly used aluminum, polyethylene, and tissue. These equivalent materials (titanium, aluminum, and tissue) are used in the realistic slabs, and the reduced error associated with the new equivalent materials is considered.

3. Results

3.1 Effects of Converting to Equivalent Aluminum, Polyethylene, and Tissue

Figures 2-4 show dose (left panes) and dose equivalent (right panes) as a function of depth for each material group exposed to the August 1972 King SPE, and Figures 5-7 show the same quantities for the 1977 solar minimum GCR environment. Dose and dose equivalent were computed in a tissue detector for all of the materials considered. For all the figures presented, the materials in the legend will be listed in decreasing order according to their value (dose or dose equivalent) at 100 g/cm^2. The equivalent material in each group (aluminum, polyethylene, or tissue) will be the only line with a symbol. The rise in dose equivalent shown in the right pane of Figure 5 for stainless steel, copper, and titanium is due to neutron buildup. At depths larger than 100 g/cm^2, the neutron dose equivalent will reach a peak value and then decline with neutron production. The depth and magnitude of the peak depends on the material and radiation environment.

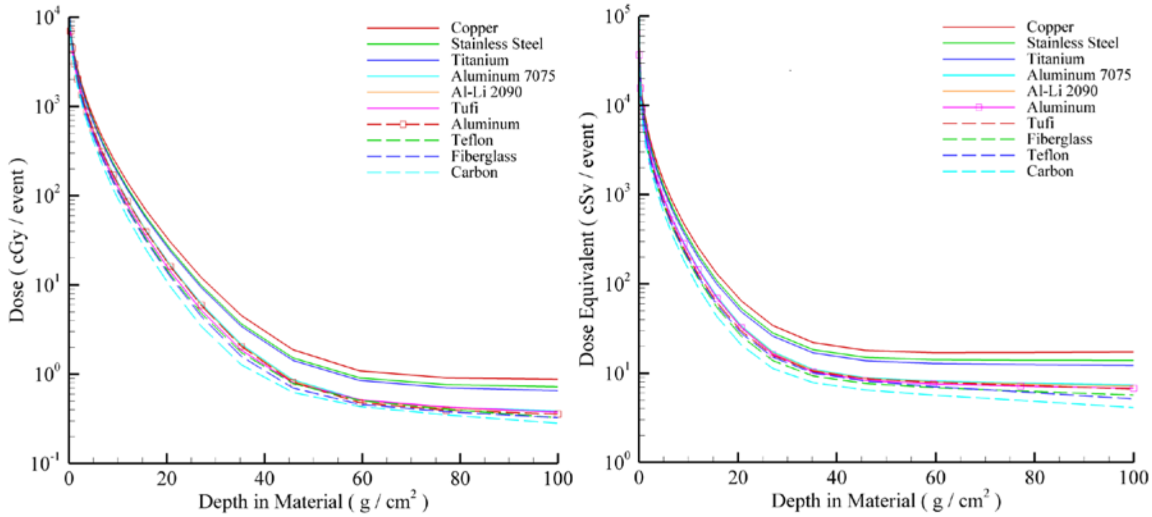

Figure 2. Dose (left pane) and dose equivalent (right pane) versus depth for materials in the aluminum group exposed to the August 1972 King SPE.

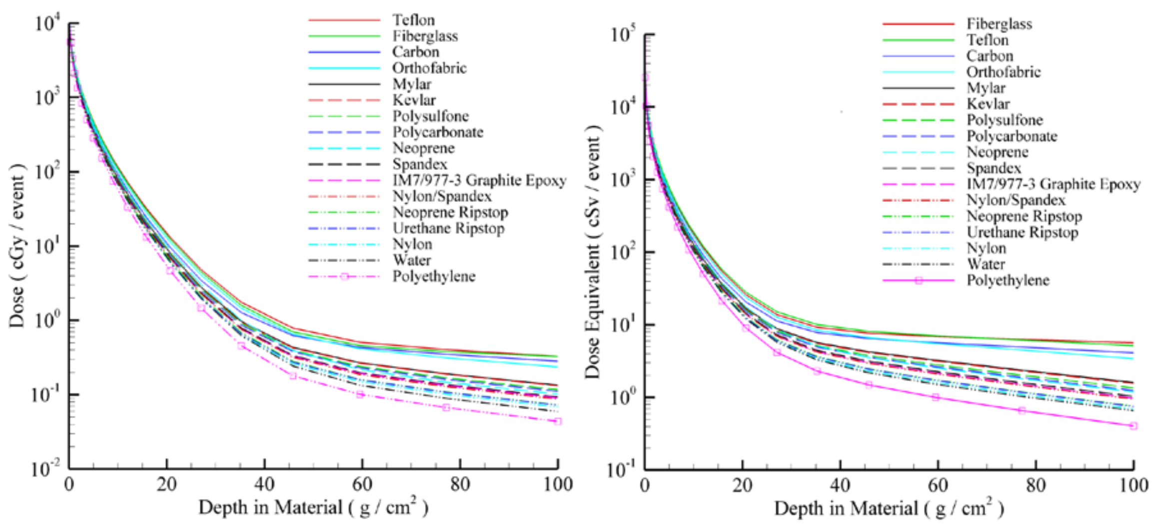

Figure 3. Dose (left pane) and dose equivalent (right pane) versus depth for materials in the polyethylene group exposed to the August 1972 King SPE.

The error for the equal thickness approximation can be quantified in the following way. Let $Y_m(d)$ be the response (dose or dose equivalent) for material m at depth d and $Y_e(d)$ be the response at depth d in the equivalent material e for the group. The percent difference of the equal thickness approximation is simply

$$(Y_m(d) - Y_e(d)) \,/\, Y_m(d) \quad \% \ . \tag{1}$$

It should be noted that this is a signed percent difference; a positive value means that the approximation is smaller than the correct value, and a negative number means the approximation is larger than the correct value. It should also be mentioned that the magnitude of errors given in this paper is dependent on the choice of aluminum, polyethylene, and tissue as equivalent materials. A different choice of equivalent materials would clearly change the magnitude of errors.

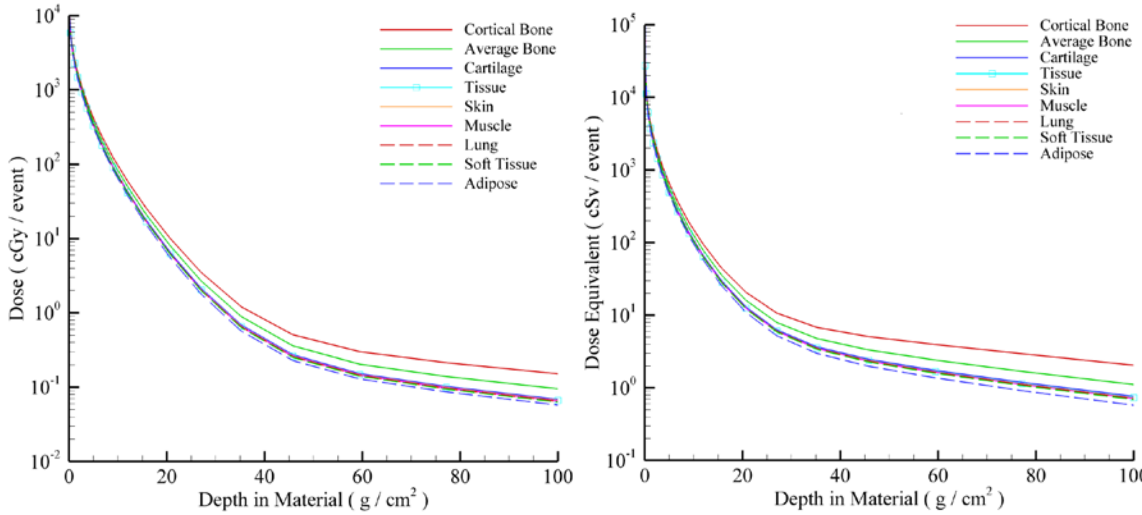

Figure 4. Dose (left pane) and dose equivalent (right pane) versus depth for materials in the tissue group exposed to the August 1972 King SPE.

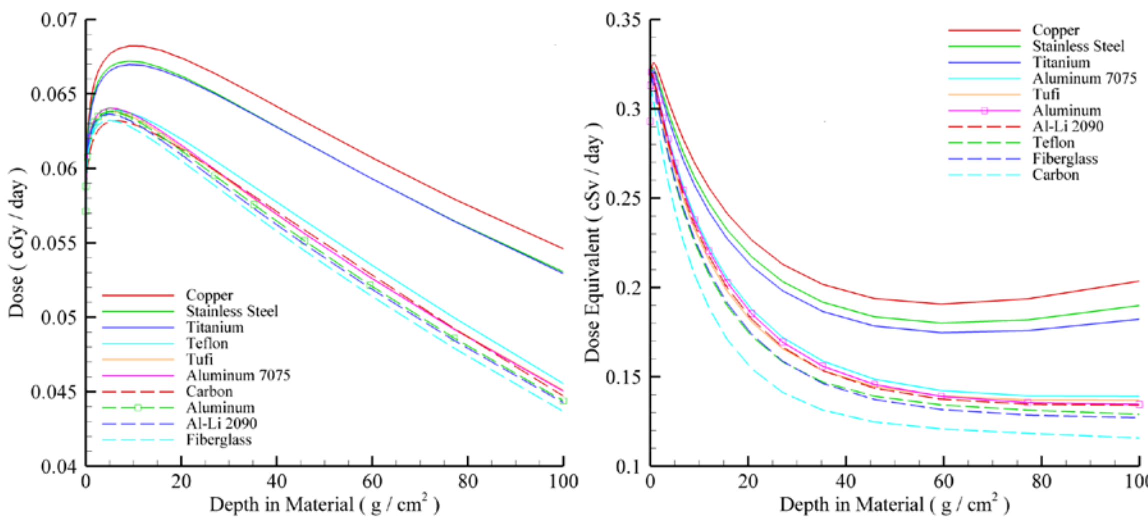

Figure 5. Dose (left pane) and dose equivalent (right pane) versus depth for materials in the aluminum group exposed to the 1977 solar minimum GCR.

As can be seen from Figures 2-7, in each group there are materials that are outliers, materials that are close to the group material, and materials in between. For simplicity, only a representative subset of the materials that cover the results in each group will be presented in the remaining figures. Figures 8-10 show the percent difference for dose equivalent for materials scaled with the equal thickness approximation in the aluminum, polyethylene, and tissue groups exposed to the August 1972 King SPE (left panes) and 1977 solar minimum GCR (right panes). The error curves for dose were similar to those shown in Figures 8-10, but with smaller magnitudes. This indicates that equal thickness scaling affects the lower energy, higher LET, particles; thereby having a greater impact on the dose equivalent values through the LET dependent quality factor. In general, the errors for the SPE environment were larger than those for the GCR environments. At these depths, the GCR exposures are dominated by heavy ions ($Z > 2$) with average momenta much larger than that of the light ions ($Z \leq 2$) that dominate SPE exposures. In this context, the high momenta of the GCR ions make the atomic structure of the target less important compared to the SPE ions, and the error associated with equal thickness scaling is reduced. It should be noted, however, that the errors for the GCR environment are still non-negligible.

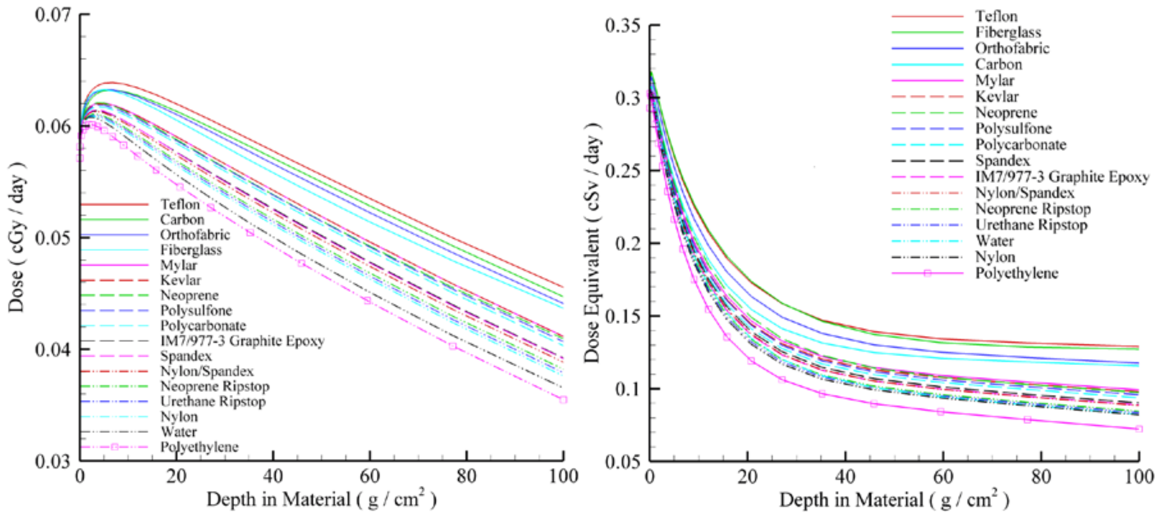

Figure 6. Dose (left pane) and dose equivalent (right pane) versus depth for materials in the polyethylene group exposed to the 1977 solar minimum GCR.

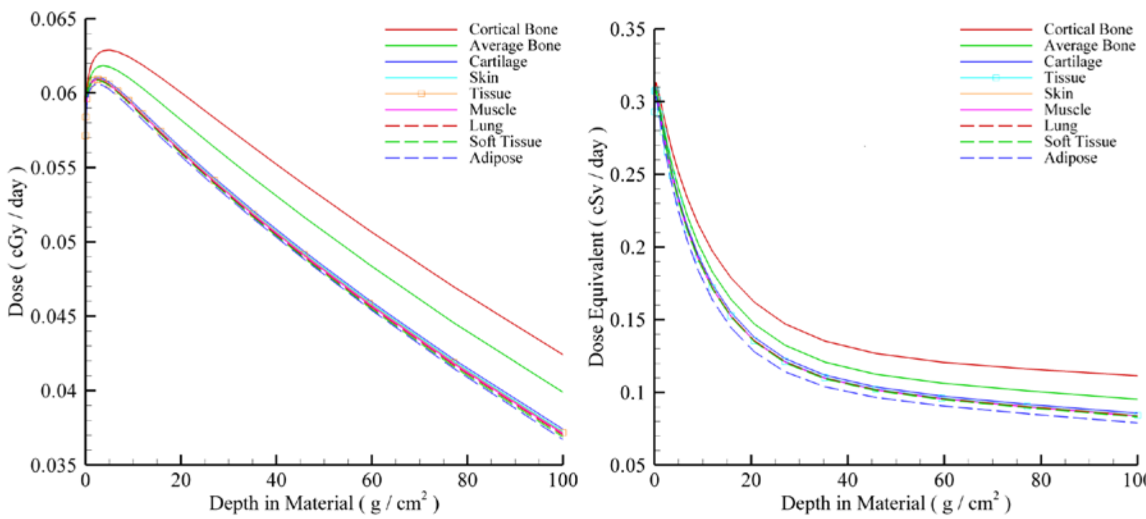

Figure 7. Dose (left pane) and dose equivalent (right pane) versus depth for materials in the tissue group exposed to the 1977 solar minimum GCR.

Alternatively, the atomic and nuclear structure of the target plays a larger role, if one considers the errors within each group separately. For example, the errors for SPE and GCR within the aluminum group are minimized as the average charge of the material comes closer to aluminum, indicating the importance of target fragmentation in high *Z* targets. In the polyethylene group, the errors are minimized if a significant amount of hydrogen is present in the target material, as can be seen by noticing that water has the smallest error in the group. Finally, in the tissue group, the largest errors occur for the bone materials and adipose. The errors for bone are caused by the increased presence of high *Z* atoms (calcium) in the material. These high *Z* targets lead to increased nucleon production and therefore change the spectrum of particles depositing energy at the target point. The errors for adipose are negative because of a lack of high *Z* atoms and increased hydrogen content compared to tissue, both of which contribute to reducing exposure quantities.

In general, it can be seen in Figures 8-10 that the errors in the equal thickness approximation roughly trend with the difference between the average charge of the target material and the average charge of the equivalent material. The trend is that the materials with a larger average charge have positive errors, those with a smaller average charge have negative errors, and the magnitude of the errors becomes greater with the magnitude of the differences in charge. This indicates that fragmentation is the largest source of error in the equal thickness approximation. It is important to remember that when extrapolating the errors in Figures 8-10 to a full vehicle, habitat, or human phantom geometry, the errors are to be weighted with the dose or dose equivalent value at that depth and then integrated over all of the vehicle thicknesses. This weighting means that a small error on a very large value can have more impact than a large error on a very small value, and the total error for a vehicle is a complex mix of each contributing error. In the case of an SPE environment, the total exposure is heavily dominated by thinly shielded regions, and therefore the error associated with equal thickness scaling, which is small at such depths will be reduced significantly.

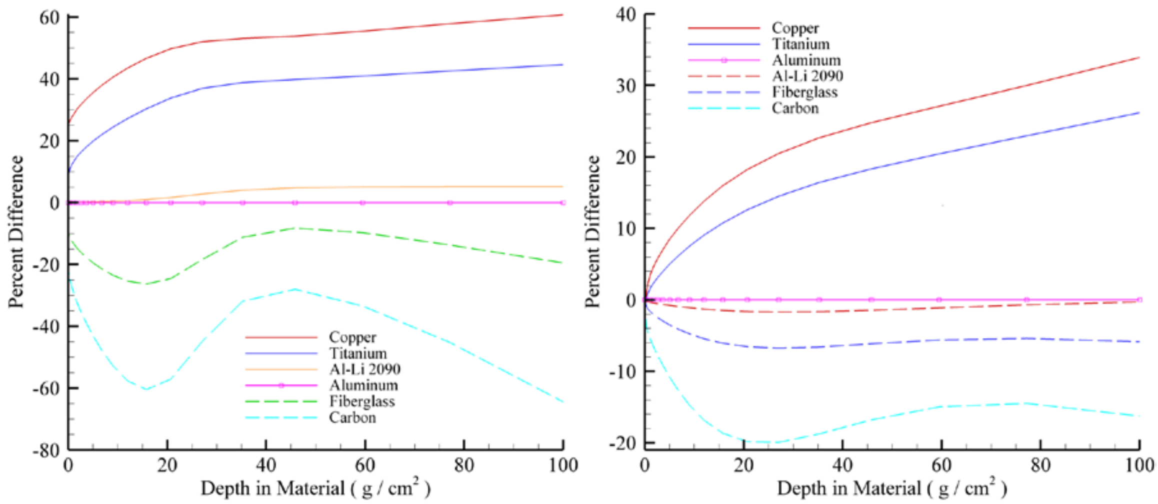

Figure 8. Percent difference for dose equivalent for materials scaled with the equal thickness approximation in the aluminum group exposed to the August 1972 King SPE (left pane) and 1977 solar minimum GCR (right pane).

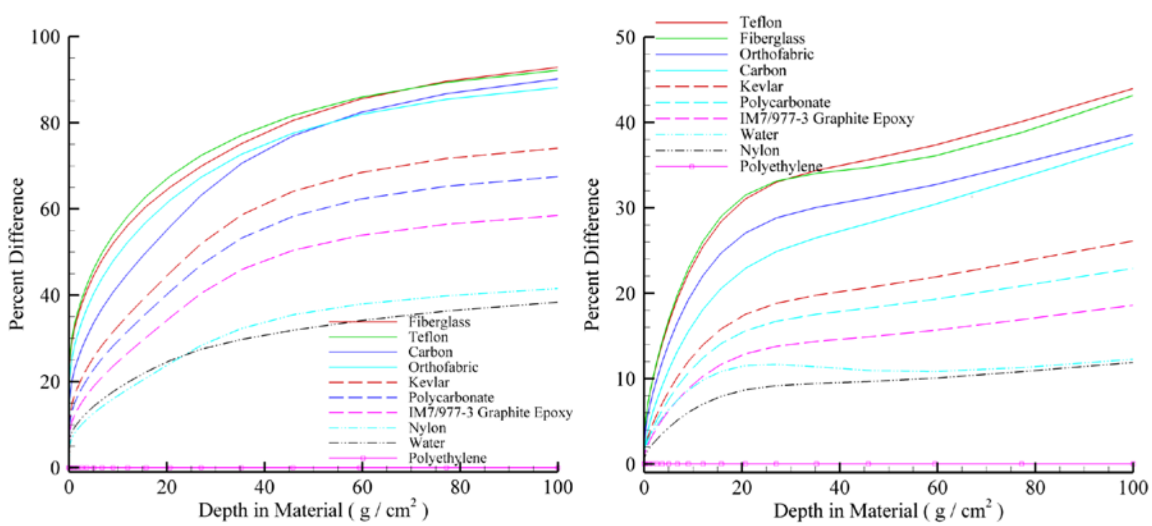

Figure 9. Percent difference for dose equivalent for materials scaled with the equal thickness approximation in the polyethylene group exposed to the August 1972 King SPE (left pane) and 1977 solar minimum GCR (right pane).

Now, consider the effects of utilizing range scaling to convert to equivalent materials. Let $Y_m(d)$ be defined as above, and let ρ_m be the range scaling ratio for material m. The range scaled equivalent thickness response for material m, is $Y_e(\rho_m d)$. The quantity $\rho_m d$ is the range scaled depth in the equivalent material. Range scaling values for each of the materials considered here can be found in Table 1. The percent difference for range scaling a material into an equivalent material is calculated by replacing $Y_e(d)$ with $Y_e(\rho_m d)$ in equation (1).

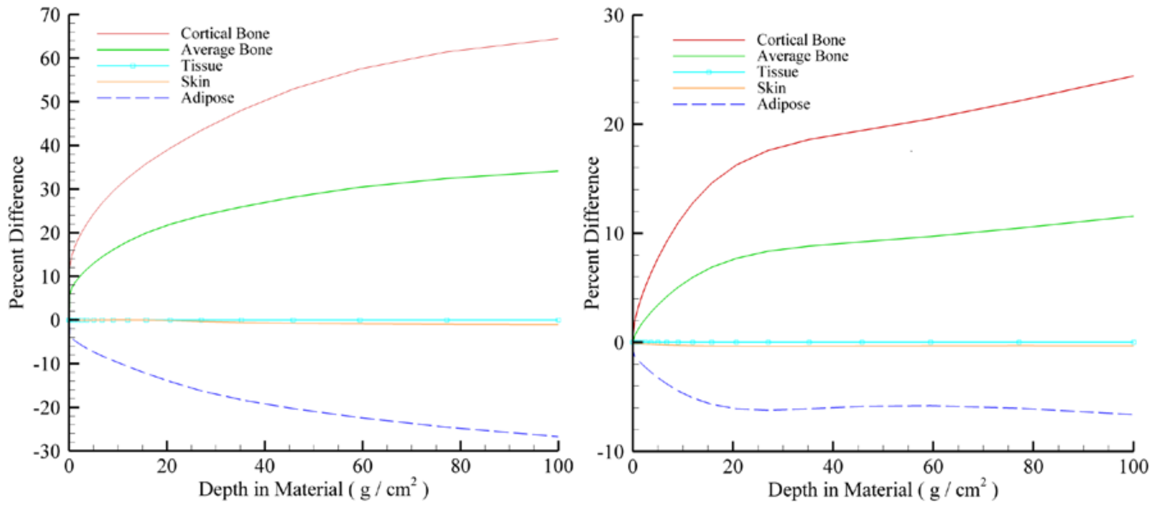

Figure 10. Percent difference for dose equivalent for materials scaled with the equal thickness approximation in the tissue group exposed to the August 1972 King SPE (left pane) and 1977 solar minimum GCR (right pane).

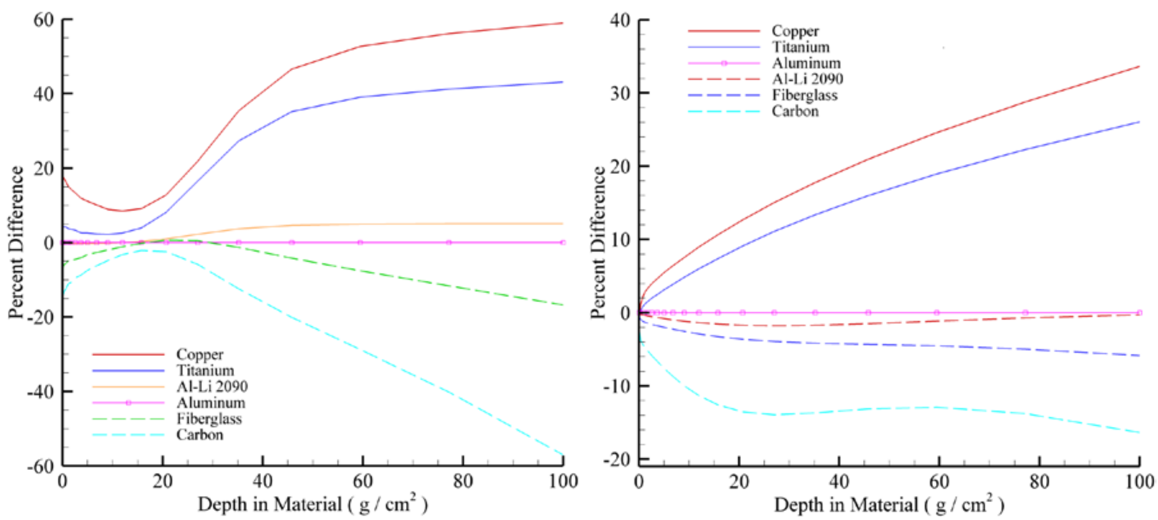

Figure 11. Percent difference for dose equivalent for materials scaled with the range scaling approximation in the aluminum group exposed to the August 1972 King SPE (left pane) and 1977 solar minimum GCR (right pane).

Figures 11-13 show the percent difference for dose equivalent for materials scaled with the range scaling approximation in the aluminum, polyethylene, and tissue groups exposed to the August 1972 King SPE (left panes) and 1977 solar minimum GCR (right panes). In general, the results shown in Figures 11-13 have very similar trends to what was shown in Figures 8-10. The errors for the SPE exposures are larger than for the GCR exposures. The errors also still seem to be trending roughly with the difference between the average nuclear charge of the target material and the average nuclear charge of the equivalent material. Also, comparing Figure 8 with Figure 9 and Figure 11 with Figure 12, it is concluded that carbon, fiberglass, and Teflon are better approximated by equivalent aluminum than by equivalent polyethylene.

Figures 11-13 allow the possible benefits of the range scaling approximation to be quantified. It is well known that SPE exposures over the first ~30 g/cm^2 of shielding are dominated by primary protons with energy less than 200 MeV. In this case, the use of range scaling with R_{50} values leads to reduced scaling errors. This is reflected in the left panes of Figures 11-13, where the errors in Figures 8-10 are reduced over the first 30 g/cm^2 by as much as 58% for the aluminum group (carbon), 50% for the polyethylene group (Teflon), and 30% for the tissue group (cortical bone). At depths larger than 30 g/cm^2, energy deposition becomes increasingly dependent on secondary particle production, and the use of range scaling becomes less important. Conversely, GCR exposures over the depths considered here are dominated by heavy ions, as discussed previously. In this case, the use of R_{50} values in range scaling affords no noticeable reduction in scaling error, as shown in the right panes of Figures 8-13. Again, it is important to remember that when extrapolating the errors in Figures 8-13 to full geometries, the errors should be weighted with the dose or dose equivalent values at that depth and then integrated over all of the vehicle thicknesses. The significant reduction in error afforded by range scaling at small shielding thicknesses is therefore significant for SPE exposures, and less important for GCR exposures. In general, it is concluded that range scaling is a more accurate approximation than equal thickness scaling

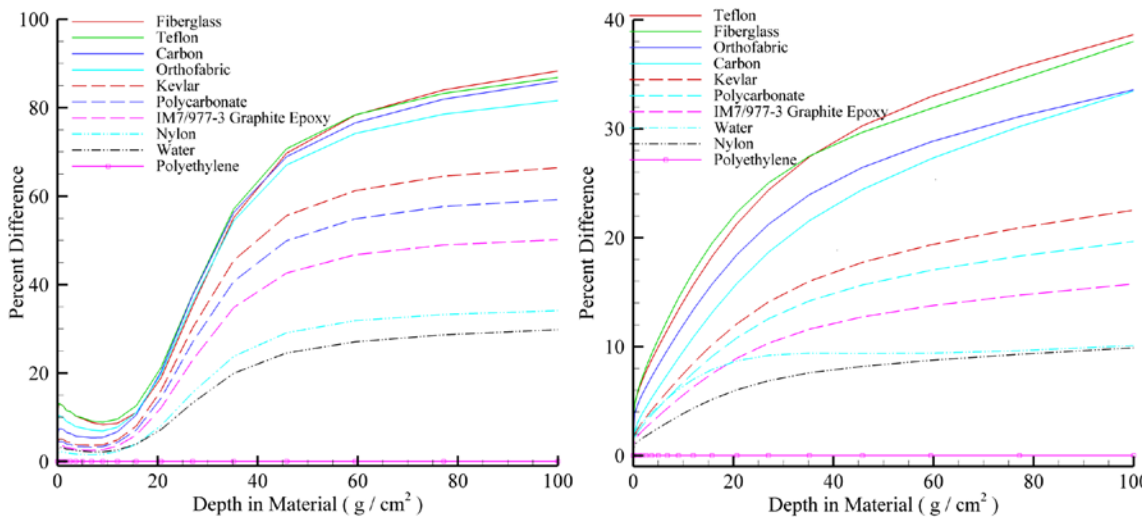

Figure 12. Percent difference for dose equivalent for materials scaled with the range scaling approximation in the polyethylene group exposed to the August 1972 King SPE (left pane) and 1977 solar minimum GCR (right pane).

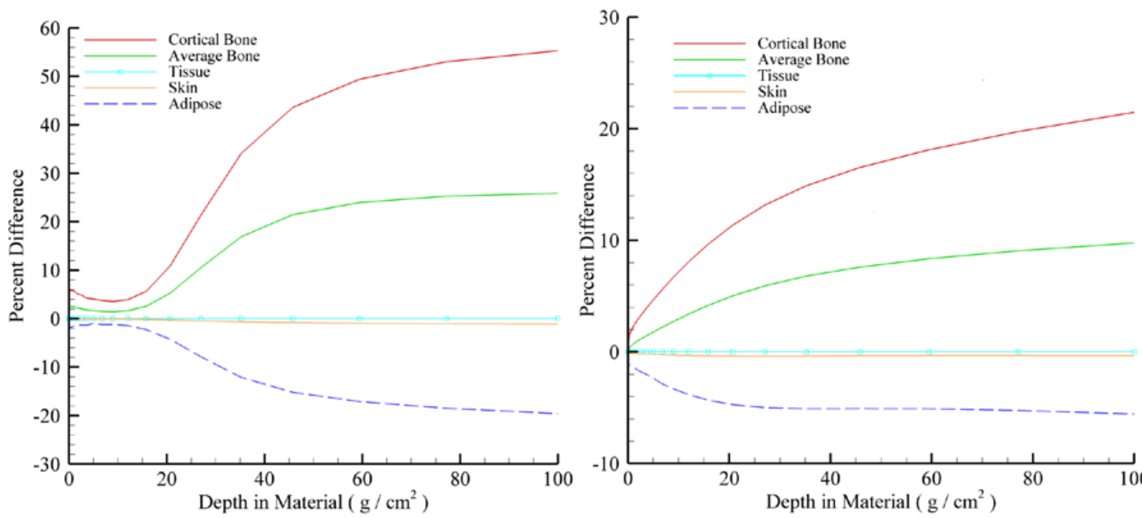

Figure 13. Percent difference for dose equivalent for materials scaled with the range scaling approximation in the tissue group exposed to the August 1972 King SPE (left pane) and 1977 solar minimum GCR (right pane).

3.2 Effects of Reordering Materials

Tables 2 and 3 show reordering errors for dose equivalent for multi-layer slabs of AT and PT exposed to the August 1972 King SPE. Tables 4 and 5 show the results for the same slabs exposed to the 1977 solar minimum GCR. Results for the AP slabs are not shown because of the similarity to the AT results. Results for dose show similar trends to what is shown in Tables 2-5 but with smaller errors, as discussed in the previous section. In Tables 2-5, the first column on the left indicates the total thickness of the slab being considered. The second column is the reference dose equivalent value for the error comparison. The remaining columns are the percent difference of the results behind multi-layer slabs to the reference results. For the AT slabs, the reference value was the dose equivalent (H60) behind the 2-layer AT arrangement. For the PT slabs, the reference value was the dose equivalent behind the 2-layer PT arrangement. Recall that this convention was chosen because in most shielding scenarios, the tissue thicknesses are always behind shielding (shielded astronaut), and multi-layer slabs or rays are collapsed to 2-layer arrangements in the ray-tracing or interpolation procedures.

For the SPE results, reordering errors are bounded above by 43%, and the errors generally increase with the slab thickness and number of layers being reordered, as expected. For the GCR results in Tables 4 and 5, reordering errors are bounded by 7%, and the same trends with slab thickness and number of layers are evident. Tables 3 and 5 show that reordering error for polyethylene and tissue is almost negligible compared to reordering error for aluminum and tissue. This is primarily caused by the fact that both polyethylene and tissue are hydrogenous and contain only low percentages of high Z atoms. This also explains why the results for the AP arrangements were very similar to the AT arrangements.

As stated previously, the errors shown in Tables 2 and 3 should be taken carefully. In a complex vehicle or habitat structure, rays will traverse many material types while passing through the shielding. Thus, the total error introduced by material reordering will be obtained by integrating the errors in Tables 2-5 over a complex distribution of thicknesses and number of layers being reordered in multiple ways. It is expected that the errors shown in Tables 2-5 give reasonable bounds on reordering errors.

Table 2. Reordering error for dose equivalent (H60 in units of cSv/event) for multi-layer slabs of AT exposed to the August 1972 King SPE. The reference value used was the dose equivalent behind a 2-layer AT slab (second column from the left). The number of layers is indicated in the second heading row.

Thickness	H60	AT reordering error (%)				
(g/cm^2)	(cSv/event)	4	8	16	32	64
1.0	4943.07	0.6	1.0	1.3	1.9	2.3
10.0	142.58	0.2	0.5	1.4	2.5	2.9
50.0	2.70	6.5	11.9	18.0	22.6	36.4
100.0	0.84	6.9	15.5	24.4	34.8	42.8

Table 3. Reordering error (%) for dose equivalent (H60 in units of cSv/event) for multi-layer slabs of PT exposed to the August 1972 King SPE. The reference value used was the dose equivalent behind a 2-layer PT slab (second column from the left). The number of layers is indicated in the second heading row.

Thickness	H60	PT reordering error (%)				
(g/cm^2)	(cSv/event)	4	8	16	32	64
1.0	4225.07	0.2	0.1	0.0	0.0	-0.2
10.0	95.72	-0.1	0.0	0.8	1.7	1.8
50.0	1.82	0.0	0.1	1.3	2.3	11.3
100.0	0.60	-0.8	-1.0	-0.9	0.1	1.0

Table 4. Reordering error (%) for dose equivalent (H60 in units of cSv/day) for multi-layer slabs of AT exposed to the 1977 solar minimum GCR. The reference value used was the dose equivalent behind a 2-layer AT slab (second column from the left). The number of layers is indicated in the second heading row.

Thickness	H60	AT reordering error (%)				
(g/cm^2)	(cSv/day)	4	8	16	32	64
1.0	2.78E-01	0.2	0.1	0.3	0.7	0.9
10.0	1.88E-01	0.2	0.3	0.7	1.2	1.4
50.0	1.02E-01	1.2	2.0	2.7	3.1	4.8
100.0	8.50E-02	1.9	3.8	5.1	6.1	6.7

Table 5. Reordering error (%) for dose equivalent (H60 in units of cSv/day) for multi-layer slabs of PT exposed to the 1977 solar minimum GCR. The reference value used was the dose equivalent behind a 2-layer PT slab (second column from the left). The number of layers is indicated in the second heading row.

Thickness	H60	PT reordering error (%)				
(g/cm^2)	(cSv/day)	4	8	16	32	64
1.0	2.73E-01	0.0	-0.3	-0.5	-0.6	-0.8
10.0	1.70E-01	0.1	0.1	0.3	0.6	0.3
50.0	9.31E-02	-0.2	-0.3	-0.2	0.0	1.1
100.0	7.93E-02	-0.5	-0.8	-0.9	-0.7	-0.5

3.3 Combined Effects of Scaling and Reordering in Realistic Slabs

In order to investigate the combined effects of material scaling and reordering, multilayered slabs are used. These spacecraft slabs are complex, multi-layer slabs composed of various sub-layers of materials commonly used in space vehicles and habitats. The total thicknesses of the spacecraft slabs are chosen to cover a range of thicknesses from ~1g/cm^2 to ~ 100 g/cm^2. The number of sub-layers are from 3-75, and generally increased with slab thickness. The results from a representative subset will be presented.

Tables 6 and 7 show dose equivalent values, scaling errors, reordering errors, and combined scaling and reordering errors for realistic spacecraft slabs exposed to the August 1972 King SPE and 1977 solar minimum GCR. The scaling convention used was range scaling, because this approach was shown to be slightly more accurate in Section 3.1 than equal thickness scaling. Carbon, fiberglass, and Teflon were all scaled into the aluminum group based on the results in Section 3.1 as well. These materials were shown to produce smaller scaling errors if converted into equivalent aluminum instead of equivalent polyethylene. In Tables 6 and 7, the first column on the left indicates the number of material layers in the slab prior to scaling and reordering. The second column is the total original slab thickness in g/cm^2. The next three columns are the dose equivalent values behind the original, scaled, and scaled-reordered slabs. The final three columns are the errors. The "Scaling Error" column compares the results behind the original slab to the results behind the scaled slab. The "Reordering Error" column compares the results behind the scaled slab to the scaled and reordered slab. The "Total Error" column compares the results behind the original slab to the results behind the scaled and reordered slab. The sum of the scaling error and reordering error is slightly more than the total error. This slight difference is caused by the coupling of the scaling error and reordering error and is small in all cases. The results for dose are not shown because the errors show similar trends with smaller magnitudes, as indicated previously.

As in the previous sections, the errors for the SPE case are generally larger than the errors for the GCR case. The scaling errors for the SPE case are bounded by 20% and generally increase with slab thickness. The scaling errors for the GCR case are bounded by 3% but still increase with slab thickness. The reason for the difference in the bound on the scaling errors can be inferred from Figures 11 and 12. In Figure 11, the over and under estimates for material scaling generate more canceling errors for the GCR environment than for the SPE environment. Also, the errors for the GCR environment are smaller than the SPE environment. The reordering errors for the SPE and GCR cases show no general correlation with slab thickness or with the number of material layers, and the reordering errors generally account for more than half of the total error. Though these results would seem to be in conflict with the results in Section 3.2, where reordering errors were shown to be well correlated with slab thickness and number of material layers, it should be noted that the slabs in Section 3.2 were highly simplified compared to those in Tables 6 and 7. This further illustrates the point that extrapolating the errors shown in Sections 3.1 and 3.2 is very difficult in complex geometries where slabs are comprised of a distribution of materials, thicknesses, and number of layers. The average total (scaling and reordering) error for the realistic slabs examined here is 19% for the SPE environment and 11% for the GCR environment. Since these slabs cover thicknesses from 0.85 g/cm^2 to 101.44 g/cm^2, it is expected that these averages are representative of the errors one might see in a complete vehicle.

Table 6. Combined effects of scaling and reordering in realistic spacecraft slabs exposed to the August 1972 King SPE. The equivalent materials used were aluminum, polyethylene, and tissue.

Layers	Thickness (g/cm^2)	Original (cSv/event)	Scaled (cSv/event)	Scaled-Reordered (cSv/day)	Scaling Error (%)	Reordering Error (%)	Total Error (%)
3	0.85	6.73E+03	6.72E+03	5.72E+03	0.1	14.9	15.0
3	0.94	5.44E+03	5.44E+03	5.44E+03	-0.1	0.0	-0.1
7	17.45	2.75E+01	2.69E+01	2.31E+01	2.5	13.9	16.1
13	25.02	1.56E+01	1.52E+01	1.31E+01	3.1	13.6	16.2
40	27.03	1.44E+01	1.32E+01	1.16E+01	8.4	12.2	19.5
16	55.02	3.20E+00	2.58E+00	2.10E+00	19.5	18.5	34.4
17	72.27	2.91E+00	2.59E+00	2.38E+00	11.1	8.0	18.3
18	87.24	2.06E+00	1.85E+00	1.68E+00	10.5	8.9	18.5
21	101.44	4.37E+00	3.76E+00	3.05E+00	14.0	18.9	30.2

Table 7. Combined effects of scaling and reordering in realistic spacecraft slabs exposed to the 1977 solar minimum GCR. The equivalent materials used were aluminum, polyethylene, and tissue.

Layers	Thickness (g/cm^2)	Original (cSv/day)	Scaled (cSv/day)	Scaled-Reordered (cSv/day)	Scaling Error (%)	Reordering Error (%)	Total Error (%)
3	0.85	3.14E-01	3.13E-01	2.95E-01	0.2	5.7	5.9
3	0.94	2.96E-01	2.96E-01	2.96E-01	-0.1	0.0	-0.1
7	17.45	1.67E-01	1.67E-01	1.43E-01	-0.3	14.6	14.3
13	25.02	1.63E-01	1.64E-01	1.38E-01	-0.6	15.5	15.0
40	27.03	1.65E-01	1.61E-01	1.35E-01	2.5	15.7	17.8
16	55.02	1.20E-01	1.20E-01	1.03E-01	0.2	13.8	14.0
17	72.27	1.19E-01	1.19E-01	1.02E-01	0.5	13.7	14.1
18	87.24	1.13E-01	1.13E-01	9.71E-02	0.4	13.7	14.1
21	101.44	1.04E-01	1.03E-01	9.60E-02	1.7	6.5	8.0

In Tables 8 and 9, the same realistic slabs were converted into equivalent titanium, aluminum, and tissue. Other equivalent material groups and alternative material arrangements were tried in an attempt to reduce the total error, but equivalent titanium, aluminum, and tissue was found to be the best combination of materials and arrangement. Titanium (Z = 22), aluminum (Z = 13), and tissue (average Z = 3.45, 62% hydrogen) cover a large portion of the range of atomic species that are found in high percentages in spacecraft materials. These equivalent materials were chosen based on the results in Section 3.1, where the scaling errors were shown to depend primarily on the difference between the average charge of the actual material and the average charge of the equivalent material. The same trends shown in Tables 6 and 7 are once again evident in Tables 8 and 9. The GCR errors are generally smaller than the SPE errors. The scaling errors for the SPE case tend to increase with slab thickness, and the reordering errors dominate the total error in most cases. Most importantly, the average total error for the SPE case has been reduced from

19% to 7%, and the average total error for the GCR case has been reduced from 11% to 7%. Though only a modest improvement, such gains in accuracy can potentially translate into non-negligible changes in shielding mass and significant changes in mission cost.

Table 8. Combined effects of scaling and reordering in realistic spacecraft slabs exposed to the August 1972 King SPE. The equivalent materials used were titanium, aluminum, and tissue.

Layers	Thickness (g/cm^2)	Scaled (cSv/event)	Scaled-Reordered (cSv/day)	Scaling Error (%)	Reordering Error (%)	Total Error (%)
3	0.85	6.73E+03	5.90E+03	-0.1	12.4	12.3
3	0.94	5.60E+03	5.60E+03	-2.9	0.0	-2.9
7	17.45	2.72E+01	2.44E+01	1.3	10.1	11.3
13	25.02	1.55E+01	1.41E+01	1.0	9.1	10.0
40	27.03	1.44E+01	1.57E+01	0.0	-9.3	-9.3
16	55.02	2.72E+00	2.20E+00	14.9	19.2	31.3
17	72.27	2.66E+00	2.45E+00	8.5	8.1	16.0
18	87.24	1.89E+00	1.73E+00	8.3	8.7	16.3
21	101.44	4.58E+00	5.36E+00	-4.8	-16.9	-22.5

Table 9. Combined effects of scaling and reordering in realistic spacecraft slabs exposed to the 1977 solar minimum GCR. The equivalent materials used were titanium, aluminum, and tissue.

Layers	Thickness (g/cm^2)	Scaled (cSv/day)	Scaled-Reordered (cSv/day)	Scaling Error (%)	Reordering Error (%)	Total Error (%)
3	0.85	3.14E-01	3.02E-01	0.0	3.7	3.7
3	0.94	3.02E-01	3.02E-01	-2.3	0.0	-2.3
7	17.45	1.71E-01	1.54E-01	-2.4	9.8	7.6
13	25.02	1.65E-01	1.48E-01	-1.5	10.4	9.1
40	27.03	1.66E-01	1.49E-01	-0.9	10.5	9.7
16	55.02	1.20E-01	1.04E-01	-0.2	13.7	13.5
17	72.27	1.19E-01	1.03E-01	0.3	13.6	13.9
18	87.24	1.13E-01	9.74E-02	0.3	13.6	13.9
21	101.44	1.15E-01	1.09E-01	-10.3	5.1	-4.7

4. Conclusions and Future Work

In this work, the error associated with converting common spacecraft materials into equivalent materials and the effects of reordering were investigated. The accuracy of using equivalent materials, irrespective of the scaling used, depends on the choice of equivalent material. It was shown that the scaling error depends heavily on the difference between the average charge of the actual material and average charge of the equivalent material. Scaling errors are minimized if equivalent materials can be chosen near the actual materials on the periodic table. It was also shown that range scaling is more accurate than equal thickness scaling in the cases considered. For SPE exposures, scaling errors were reduced by anywhere from 30% to 58% for shielding thicknesses less than 30 g/cm^2 if range scaling is used. For thicker shields, or for GCR exposures, range scaling offered little improvement over equal thickness scaling due to the increased importance on fragmentation. The error associated with reordering materials was also examined. In simple cases, with specific materials and specific thicknesses, the errors can be shown to increase with material thickness and the number of layers. In more realistic slab examples, reordering errors are not well correlated with total slab thickness or number of layers due to the increase complexity of the layer thicknesses and material types found in realistic spacecraft slabs. The more realistic slabs studied here indicated that reordering error accounts for more than half of the total error, in general. For the realistic slabs considered here, the average total (scaling plus reordering) error was 19% for the SPE case and 11% for the GCR case. When the equivalent materials were switched from aluminum, polyethylene, and tissue to titanium, aluminum, and tissue, these errors were reduced to 7% for the SPE case and 7% for the GCR case. Future work will quantify these errors in complete vehicle geometries by transporting through every ray in the vehicle ray-trace.

5. References

Badavi, F.F., Adams, D.O., Wilson, J.W., On the Validity of the Aluminum Equivalent Approximation in Space Radiation Shielding Applications. Advances in Space Research, Volume 46, pp. 719-727 (2010).

International Commission on Radiological Protection, 1990 Recommendations of the International Commission on Radiological Protection. ICRP Publication 60, Pergamon (1990).

King, J.H., Solar Proton Fluences for 1977-1983 Space Missions. Journal of Spacecraft and Rockets, Volume 11, pp. 401-408 (1974).

O'Neill, P.M., Badhwar-O'Neill Galactic Cosmic Ray Model Update Based on Advanced Composition Explorer (ACE) Energy Spectra from 1997 to Present. Advances in Space Research, Volume 37, pp. 1727-1733 (2006).

Slaba, T.C., Blattnig, S.R., Badavi, F.F., Faster and more Accurate Transport Procedures for HZETRN. Journal of Computational Physics, Volume 229, pp. 9397-9417 (2010).

Wilson, J.W., Townsend, L.W., Schimmerling, W., Khandelwal, G.S., Khan, F., Nealy, J.E., Cucinotta, F.A., Simonsen, L.C., Shinn, J.L., Norbury, J.W., Transport Methods and Interactions for Space Radiations. NASA Reference Publication 1257 (1991).

Wilson, J.W., Tripathi, R.K., Mertens, C.J., Blattnig, S., Clowdsley, M.S., Cucinotta, F.A., Tweed, J., Heinbockel, J.H., Walker, S.A., Nealey, J.E., Verification and Validation: High Energy and Charge (HZE) Transport Codes and Future Development. NASA Technical Paper 213784 (2005).